Environmental Modelling & Software 110 (2018) 62–71

Contents lists available at ScienceDirect

Environmental Modelling & Software

journal homepage: www.elsevier.com/locate/envsoft

Inverse modelling of snow depths

Uwe Schlink*, Daniel Hertel

Dept. Urban and Environmental Sociology, Helmholtz Centre for Environmental Research – UFZ, Permoserstr. 15, D-04318 Leipzig, Germany

ARTICLE INFO

Article history:
Received 7 February 2017
Received in revised form
13 October 2017
Accepted 13 January 2018
Available online 9 February 2018

Keywords:
Bayesian estimation
Operational snow forecasting
Prediction performance
Sub-alpine snow cover
ESCIMO model

ABSTRACT

Operational snow forecasting models contain parameters for which site-specific values are often unknown. As an improvement a Bayesian procedure is suggested that estimates, from past observations, site-specific parameters with confidence intervals. It turned out that simultaneous estimation of all parameters was most accurate. From 2.5 years of daily snow depth observations the estimates were for snow albedo 0.94, 0.89, and 0.56, for snow emissivity 0.88, 0.92, and 0.99, and for snow density (g/cm^3) 0.14, 0.05, and 0.11 at the German weather stations Wasserkuppe, Erfurt-Weimar, and Artern, respectively. Using estimated site-specific parameters, *ex post* snow depth forecasts achieved an index of agreement IA = 0.4–0.8 with past observations; IA = 0.3–0.8 for a 51-years period. They outperformed the precision of predictions based on default parameter values (0.1 < IA<0.3). The developed inverse approach is recommended for parameter estimation and snow forecasting at sub-alpine stations with more or less urban impact and for application in education.

© 2018 Elsevier Ltd. All rights reserved.

1. Introduction

In alpine regions as well as in subalpine mountainous areas ski tourism is an important factor for regional economy. Depending on fluctuations in atmospheric circulation patterns (so-called weather types (Hess and Brezowsky, 1969; Lamb, 1950)) the snow cover can vary considerably between the months and years. The snow-reliability is also threatened by climate change (Marke et al., 2015). In order to ensure a sufficient snow depth, artificial snow-making is common practice (Schmidt et al., 2012) and this calls for support by suitable snow models and forecasting procedures.

Besides these needs of winter tourism, snow modelling has much broader relevance to many applications, such as avalanche risk warning (Bartelt and Lehning, 2002), hydrological (flood predictions and hydropower (Leisenring and Moradkhani, 2011),) and weather forecasting (Mauser and Bach, 2009). Detailed snowpack schemes have been developed for inclusion into numerical weather prediction and climate models (Vionnet et al., 2012) and involve a more or less explicit description of the time evolution of snow microstructure.

Simpler snow schemes consider the snowpack as a single layer (Etchevers et al., 2004). The processes in the interior of the snowpack and the interactions with the surroundings are described by balance equations. They are parameterized featuring specific properties, such as a high albedo, fixed density, a low thermal capacity and low thermal conductivity. An advantage of such single-layer models is that they capture first order processes. This makes them pertinent for application in education, for on-site demonstrations and visualizations of the simulated snow cover directly in the field (Marke et al., 2016). Even local authorities show interest to run such simple and inexpensive models that can quickly provide estimates and forecasts during discussions with local snowmaker operators.

Due to their low complexity the performance of single-layer models is limited. Improvement might be possible when site-specific model parameters are used instead of usually applied default values. An adequate technique for the estimation of parameters is inverse modelling that can estimate model parameters from a set of observational data (Aster et al., 2013). For an assessment of parameter uncertainties, the utilization of Bayesian inference is helpful. For the model parameters to be estimated, this method iteratively updates a non-informative a priory probability distribution according to Bayes' theorem and utilizing the information contained in the observational data. After convergence of this repeated procedure, the data of the updated model parameters are sampled to obtain their posterior probability distribution (Spiegelhalter and Rice, 2009).

The application of Bayesian inference is particularly straightforward for a hierarchical statistical model. For an outcome variable (such as the snow depth), a hierarchical model represents its

* Corresponding author.
E-mail address: uwe.schlink@ufz.de (U. Schlink).

https://doi.org/10.1016/j.envsoft.2018.01.010
1364-8152/© 2018 Elsevier Ltd. All rights reserved.

dependence on more than one independent random variables. For example, the outcome 'snow depth' depends on the parameter 'snow density' in a different way than on the parameter 'snow albedo'. These relationships are represented by the equations of the hierarchical model (see equations (1–12) below and their explanation).

The present study utilizes the physically based point snow surface model (Energy balance Snow Cover Integrated MOdel - ESCIMO) that has been developed (Strasser et al., 2002) and implemented in a spreadsheet (ESCIMO.spread (Strasser and Marke, 2010)) as an easy-to-use and portable software tool for the hourly simulation of the energy balance, the water equivalent and melt rates of a snow cover. This one-dimensional approach assumes the snow cover to be a single and homogeneous pack and solves the energy and mass balance equations for the snow surface assuming simple parameterizations of the relevant processes.

The outcome variable of ESCIMO is the snow water equivalent that depends on a set of parameters. While some of them are physical constants (such as the specific heat of snow or the melting heat of ice), others strongly refer to the situation that is under consideration. The latter comprise (Strasser and Marke, 2010) the soil heat flux, snow albedo, emissivity of snow, clear sky emissivity, density of snow, a recession factor characterizing the albedo changes during ageing of snow, the threshold snowfall needed for the albedo to switch from old (aged) to new snow, a temperature threshold for detection of the precipitation phase (liquid or solid), and two parameters relating sensible and latent heat flux to wind speed (Kuchment and Gelfan, 1996).

Many of the model parameters can be derived from site measurements or from remote sensing data, applying the AMUNDSEN (Alpine Multiscale Numerical Simulation Engine) software tool, for example for the specification of the snow albedo (Strasser et al., 2004). Such specification procedures involve tentative simulations that are evaluated by a comparison with observations. Best consistency of simulations and observations indicate an adequate parameter value. Parameters specified at a certain site are often transferred to other sites for want of better information.

Environmental data science can provide a remedy to the scarcity in site-specific parameters. The integration of data routinely gathered and delivered by monitoring systems (such as weather observations including snow depths) with data analysis tools facilitates the estimation of the wanted parameters for many locations and time periods. The results of the estimation procedure find their way into operational snow forecasting for the benefit of the public. So far, in this chain of data flow there is a gap because of the lack of an adequate technique providing the site-specific parameters.

Taking advantage of the ESCIMO software code, an inverse modelling approach is suggested for the estimation of model parameters from routinely observed snow data. For that purpose the ESCIMO formulas (Strasser and Marke, 2010) are re-arranged into a hierarchical model (1)–(12) for the snow depth. Due to its complexity straightforward estimation techniques (e.g. maximum likelihood) are difficult to apply, and therefore Bayesian inference is used that provides interval estimates for the model parameters. In the following the development, application and evaluation of this approach is explained for the parameters snow density, snow albedo, snow emissivity, and soil heat flux. Compared to all other model parameters, these parameters are most influenced by the considered site. Parameters representing threshold values can weaken the convergence of the Markov Chain Monte Carlo (MCMC) simulations applied for the Bayesian inference. For that reason these threshold parameters will need special consideration and are not included in the present analysis.

In this study the ESCIMO model was implemented, firstly in OpenBUGS (Lunn et al., 2009) for Bayesian parameter estimation and, secondly in R (R Core Team, 2014) for simulations. To evaluate the quality of the parameter recovery, the OpenBUGS procedure was applied to simulations calculated with pre-specified parameter values for a period of 2.5-years. As a result the bias and uncertainty of the estimates are plotted.

Next, the estimation procedure was applied to real snow depth data observed during 2.5 years and the estimated parameter values were compared. Finally, these parameters were used to make predictions for periods of 2.5 and 51 years. A set of performance measures was calculated from these *ex post* forecasts and past observations.

Our study region is the federal state of Thuringia situated in the Central German Uplands. Analyzing meteorological data measured at the stations in Erfurt-Weimar (316 m a.s.l.), Artern (164 m a.s.l.), and Wasserkuppe (912 m a.s.l.), ESCIMO is probed at sub-alpine levels and with urban influences. All data were provided by the German Weather Service (DWD, Regionales Klima informations system ReKIS). As the ESCIMO.spread model works with long-wave radiation measurements in the energy balance and these data were unavailable from the considered stations, a parameterization scheme for the long-wave radiation is suggested additionally. The contribution of long-wave radiation to the energy balance is parameterized by the snow emissivity, which is one of our estimated parameters. Further, for compatibility with the observed meteorological data, which were not available at an hourly basis, the time-basis of ESCIMO was changed from hourly to daily time steps.

Exploring the capabilities and limitations of Bayesian inverse modelling of snow depth, in our study we hypothesize that:

- environmental models can be re-arranged to a hierarchical structure to which Bayesian techniques can be applied in a straightforward manner,
- site-specific model parameters can be estimated by means of inverse modelling; they vary between sites and can differ from values given in the literature (Strasser and Marke, 2010),
- for sub-alpine sites, the estimated parameters can improve the performance of ESCIMO compared to the default parameter values suggested with ESCIMO.spread in the alpine context,
- routinely gathered meteorological data are suitable for snow depth predictions based on ESCIMO utilizing parameter estimates derived from past snow observations, and this procedure of inverse modelling can be included into operational weather forecasting systems,
- site-specific parameter estimates suggest that the accumulation of snow depends on the altitude,
- ESCIMO is applicable to both hourly and daily meteorological data.

2. Model setup and inverse modelling

The ESCIMO model is based on the energy balance (EB) of a snow pack (for details of each of the following model equations (1–12) see Strasser and Marke (2010)). Contributions to the energy balance (5) comprise the soil heat flux (B), advective energy (aS and aR, respectively) supplied by solid (S) or liquid (R) precipitation, sensible (H) and latent (E) heat fluxes, as well as short- ($(1-\alpha)G$) and long-wave (L) net radiation. On the basis of the individual terms given in detail by Strasser and Marke (2010) the energy balance is applied to melting (if air temperature $\geq$ 273.15 K) and no melt (air temperature < 273.15 K, see equation (4)) and eventually predicts the snow water equivalent (SWE in mm). Here a hierarchical statistical model is suggested for the outcome variable snow

depth ($SD = \frac{SWE}{10} \cdot \frac{\rho_W}{\rho_o}$ in cm with the density of water ρ_W, see Sturm et al. (2010)) that involves the station specific snow densities (in units of $\rho_W = 1 g/cm^3$; ρ_o for new snow, ρ_M for melting snow, ρ_s for sublimated snow, and ρ_r for frozen rain on snow cover) and is assumed to follow an exponential distribution $f_{\exp}$:

$$SD_t \sim \exp(\lambda_t),\ f_{\exp}(x,\lambda) = \begin{cases} e^{-x/\lambda}/\lambda & for \quad x \geq 0 \\ 0 & x < 0 \end{cases}, \quad E[x] = \lambda, \mathrm{var}[x] = \lambda^2, \tag{1}$$

$$\lambda_t = \begin{cases} \max(0, \widetilde{SD}_{t-1}) & for \quad SD_{t-1} > 0 \\ S_t/(10\rho_o) & \mathrm{SD}_{t-1} = 0 \end{cases}, \quad \widetilde{\mathrm{SD}}_{t-1} = SD_{t-1} + \\ +(R_t/\rho_r + S_t/\rho_o + Sub_t/\rho_s - Melt_t/\rho_M)/10, \tag{2}$$

$$Sub_t = \begin{cases} 86400\ E_t/283550 & for \quad SD_{t-1} > 0 \\ 0 & SD_{t-1} = 0 \end{cases}, \tag{3}$$

$$Melt_t = \begin{cases} \min(\widetilde{\mathrm{EB}}_t, 10\rho_M \mathrm{SD}_{t-1}) & for\ \mathrm{SD}_{t-1} > 0 \wedge \mathrm{EB}_t > 0 \\ 0 & \text{otherwise} \end{cases}, \quad \widetilde{\mathrm{EB}}_t = 86400\, EB_t/337500, \tag{4}$$

$$EB_t = B + aS_t + aR_t + H_t + E_t + (1-\alpha)G_t + L_t(\varepsilon_s), \tag{5}$$

$$B = 2.0 \tag{6}$$

$$aS_t = \begin{cases} \vartheta_t \cdot 2100 \cdot S_t/86400 & for \quad S_t > 0 \\ 0 & S_t = 0 \end{cases}, \tag{7}$$

$$aR_t = \begin{cases} \vartheta_t \cdot 4180 \cdot R_t/86400 & for \quad R_t > 0 \\ 0 & R_t = 0 \end{cases}, \tag{8}$$

$$H_t = 18.85\ (a + b \cdot u_t)\ (\vartheta_t - \vartheta_{St}), \vartheta_{St} = \min(\vartheta_t, 0), \tag{9}$$

$$E_t = 32.82\ (a + b \cdot u_t)\ (e_t - e_{St}), \quad e_t = E(\vartheta_t) \cdot relHum_t, \quad e_{St} = \begin{cases} E(\vartheta_t) & for \quad SD_t > 0 \\ 0 & \mathrm{SD}_t = 0 \end{cases}, \tag{10}$$

$$L_t = \left((1 - s_t) + \varepsilon_{cl,t} s_t\right) \cdot 5.67 \cdot 10^{-8} \cdot (\vartheta_t + 273.16)^4 - \varepsilon_s \cdot 5.67 \cdot 10^{-8} \cdot (\vartheta_{St} + 273.16)^4, \tag{11}$$

$$s_t = G_t/I_t, \varepsilon_{cl,t} = 1 - \left(1 + 4650 \frac{e_t}{\vartheta_t + 273.16}\right) \cdot \cdot \exp\left(- \left(1.2 + 3{*}4650 \frac{e_t}{\vartheta_t + 273.16}\right)^{0.5}\right), \tag{12}$$

The expectation value of snow depth (λ) results from the sum of precipitation, sublimation and melting depending on whether there was snow cover on the previous day (eq. (2)). For days without snow cover both sublimation and melting disappear (equation (3)+(4)). In case of snow cover the water equivalent of sublimation (*Sub*, equation (3)) is determined by the available latent heat (*E*, equation (10)) which in turn depends on the relative humidity (*relHum*) and convection due to wind speed (u). Equation (3) couples the latent heat (in W/m^2) to the amount of sublimated snow (in mm/(86400 s)) by help of the sublimation heat of water (283550 W/kg). Likewise, equation (4) couples the energy balance (5) to the amount of melted snow by help of the melting heat of snow (337500 W/kg). While (5) is the energy balance, (2) represents the mass balance and both are linked via sublimation and melting (equations (3) and (4)). Melting (4) occurs only when the energy balance (*EB*, equation (5)) is positive, i.e. the energy flux is directed to the surface (all energy flux densities are expressed in W/m^2). Melting (4) is limited either by the available amount of snow or by the available energy.

In the model ESCIMO.spread a constant soil heat flux of $B = 2 W/m^2$ was assumed (6), as soil heat flux measurements are scarcely available. The advective energy supplied by snow or by rainfall on snow is proportional to the amount of precipitation, the air temperature, and the specific heat of snow ($c_s = 2100 Jkg^{-1}K^{-1}$) or water ($c_w = 4200 Jkg^{-1}K^{-1}$), respectively (see equations (7)+(8); 86400 representing the number of seconds per day). The sensible heat flux (H) is expressed with wind speed (u in m/s) in (9) and, accordingly, the latent heat flux (E) is calculated in (10) where e (in hPa) is the water vapor partial pressure calculated using the Magnus formula ($E(\vartheta)$), and e_S likewise for the snow surface (Kuchment and Gelfan, 1996). The last but one term in the energy balance (5) represents the fraction $(1 - \alpha)$ of short-wave radiation (global radiation, G in $J/cm^2 = 8.64\ W/m^2$) absorbed from the snow surface (α is the albedo).

Extending the ESCIMO model that requires measurements of the incoming long-wave radiation (L), this term was parameterized using the clear sky emissivity (ε_{cl}) for the fraction of sky not covered by clouds (equation (11)). For the clear sky emissivity an empirical formula (see Prata (1996)) was used. Cloud fraction is estimated by help of the solar index (s, equation (12)) that is the ratio between measured global radiation and theoretical short-wave radiation (I_t) for clear sky conditions. This effective solar constant I_t involves the solar constant ($I_o = 1370\ W/m^2$), corrections by zenith angle (Z, with $\cos(Z_t) = \sin(\text{geographic latitude})\sin(\text{declination}) + \cos(\text{geographic latitude})\cos(\text{declination})\cos(h)$, hour angle $h = (\pi/12)(t_{noon} - t))$, declination $= 0.4102 \sin\left(\frac{2\pi}{365}(DoY - 80)\right)$, DoY = Day of the Year) and transmission coefficients (Crawford and Duchon, 1999):

$$I_t = I_o \cos(Z_t) \tau_R \tau_{pg} \tau_w \tau_a. \tag{13}$$

For the transmission coefficients we have (Atwater and Brown, 1974; McDonald, 1960; Meyers and Dale, 1983):

$$\tau_R \tau_{pg} = 1.021 - 0.084\ \sqrt{m\ (0.00949\ p + 0.051\ )}, m = 35 \cos(Z_t) \Big/ \sqrt{1224 \cos^2(Z_t) + 1}, \tag{14}$$

$$\tau_w = 1 - 0.077 (w\, m)^{0.3}, \quad \tau_a = 0.935^m \ \text{with} \tag{15}$$

air pressure p in kPa, optical air mass m at 101.3 kPa, precipitable water $w = 4650\ e/T$ for e as vapor pressure in kPa and T as air temperature in K. In the long-wave radiation balance (11), the incoming radiation is complemented by the outgoing radiation parameterized by snow-emissivity (ε_S).

A second extension of the original ESCIMO model (Strasser and Marke, 2010), which calculates the snow water equivalent (*SWE* in mm), is the conversion into snow depth (*SD*) that involves the station-specific snow density (for new snow an approximation is $\rho_0 = 0.05\ g/cm^3$, see glossar at www.dwd.de). This is taken into account in (2). Thirdly, while the original ESCIMO was working on an hourly basis (t in h), here the model was used for daily observations (for that purpose the 86400 s, representing one day, were included in (3), (4), (7), and (8)) and the meaning of all quantities changed accordingly (t in d). In the calculation (13) of the effective solar constant $t = t_{noon}$ was used.

3. Design of the study

The hierarchical model was implemented in R for the calculation of simulations and, additionally, in OpenBUGS (see details in section 6 and (Lunn et al., 2009)) for estimations. Table 1 summarizes the observational variables, parameters and constants for equations (1–12). For inverse modelling of the parameters snow density, snow albedo, snow emissivity, and soil heat flux flat priors of uniform, uniform, uniform, and exponential distributions were applied, respectively.

In a first step, aiming at a validation of the hierarchical model, daily snow depths were simulated for different values of the considered four parameters (snow density in a range of $\rho_o = \rho_M = \rho_r = \rho_s \Rightarrow \quad \rho = 0.1(0.01)0.2$, snow albedo in a range of $\alpha = 0.1(0.1)0.9$, snow emissivity in a range of $\varepsilon_s = 0.90(0.01)0.99$, and soil heat flux in a range of $B = 1.5(0.1)2.5$) and using real meteorological data for the remaining variables at three sites (Erfurt-Weimar, Artern, Wasserkuppe) for a 2.5-year period (August 2010–December 2012).

Applying the Bayesian inversion procedure (see OpenBUGS code in supporting material) to these simulated data, the specified four parameters were estimated. Finally, the estimates were compared with the original parameter values used in the simulations. From this validation the precision of the estimates and the occurrence of biases become obvious. Biases can result from dependencies between parameter estimates.

As most of the parameters are tied in with equation (5) their estimates might be biased in some combinations and for some values. To analyze the mutual interaction of these parameters, they were estimated in all 32 different combinations

(α in combination with others: $\alpha; \alpha - B; \alpha - \rho; \alpha - \varepsilon_S; \alpha - \rho - B; \alpha - \rho - \varepsilon_S; \alpha - \varepsilon_S - B; \alpha - \varepsilon_S - B - \rho$;

ρ in combination with others: $\rho; \rho - B; \rho - \alpha; \rho - \varepsilon_S; \rho - \alpha - B; \rho - \alpha - \varepsilon_S; \rho - \varepsilon_S - B; \rho - \varepsilon_S - B - \alpha$;

B in combination with others: $B; B - \rho; B - \alpha; B - \varepsilon_S; B - \alpha - \rho; B - \alpha - \varepsilon_S; B - \varepsilon_S - \rho; B - \varepsilon_S - \rho - \alpha$;

ε_S in combination with others: $\varepsilon_S; \varepsilon_S - B; \varepsilon_S - \alpha; \varepsilon_S - \rho; \varepsilon_S - \alpha - B; \varepsilon_S - \alpha - \rho; \varepsilon_S - \rho - B; \varepsilon_S - \rho - B - \alpha$) keeping the not mentioned parameters constant. For the constant parameters the ESCIMO default values were used (Table 1). The MCMC procedure run for 100.000 updates (thinning 100) with rapid convergence (stable solution after ca. 25.000, Fig. 1) for α, ρ, ε_S. For B the convergence was much poorer, i. e. the solution fluctuated always.

After model validation the Bayesian procedure was applied to observational data gathered routinely at three weather stations (Erfurt-Weimar, Artern, Wasserkuppe) and estimated the four parameters (α, ε_S, B, ρ) as well as their uncertainty for different parameter combinations. Finally, the performance of the estimation procedure and the generalizability of the model were assessed from the quality of forecasts calculated with observed data for the 2.5 years and for a 51-years period (January 1961–December 2012).

Table 1
Variables, parameters, and constants (equations (1–12)) used for simulations and validation.

variable	symbol		unit
Snow depth	SD		cm
Precipitation as snow	S		mm
Precipitation as rain	R		mm
Wind speed	u		m/s
Air temperature	ϑ		$°C$
Relative air humidity	$relHum$		%
Global radiation	G		$W\ m^{-2}$
parameter	**symbol**	**default**	**unit**
Albedo	α	0.90	–
Density of snow	ρ_o	0.05	g/cm^3
Emissivity of snow	ε_S	0.99	–
Soil heat flux	B	2.00	$W\ m^{-2}$
Threshold temperature for precipitation phase detection	T_w	275.16	K
constant	**symbol**	**value**	**unit**
Stefan-Boltzmann constant	σ	5.67×10^{-8}	$W\ m^{-2}K^{-4}$
Specific heat of snow (at 0 °C)	c_{ss}	2.10×10^3	$J\ kg^{-1}K^{-1}$
Specific heat of water (at 5 °C)	c_{sw}	4.20×10^3	$J\ kg^{-1}K^{-1}$
Melting heat of ice	c_i	3.337×10^5	$J\ kg^{-1}$
Sublimation/resublimation heat of snow (at −5 °C)	l_s	2.8355×10^6	$J\ kg^{-1}$

4. Results

4.1. Model validation

Validating the suggested inverse modelling procedure all parameter estimates were compared with the parameter values used for simulating the data. In result, the estimates deviate more or less from the exact values represented by a red line in Fig. 2. For an α value used to simulate daily snow depths during the 2.5 years, a distribution of estimated albedo values was obtained (plotted as median, 25th, and 75th percentiles in Fig. 2). This distribution clearly changed with the α used for the simulation. The distribution was also different when α was estimated jointly with other parameters. For example, the estimation of α alone and in combination with ρ and B provided the same results (likewise, results overlap for all groups involving α and ε_S). These results were similar for stations Erfurt-Weimar and Artern.

A feature that is obvious for all three stations was the occurrence of a strong bias towards larger albedo estimates if the albedo is estimated together with the snow emissivity (ε_S). In contrast, snow density and soil heat flux did not bias the albedo estimate. The dependence between the estimates $\widehat{\alpha}$ and $\widehat{\varepsilon}_S$ is a consequence of (5) where the albedo is a coefficient of global radiation (G) and snow emissivity is a coefficient of the surface temperature (ϑ_S, see equation (11)). A quantitative comparison of the terms in (5) reveals that for large albedo ($\alpha > 0.9$) the short- and the long-wave energies are similar. During clear sky conditions the radiation and surface temperature data are collinear and this generates an association between the estimates $\widehat{\alpha}$ and $\widehat{\varepsilon}_S$. Further, the bias of $\widehat{\alpha}$ was largest for Wasserkuppe and smallest for Artern. This might have been caused by different ageing of snow due to differences in altitude (ca. 800 m) and short-wave radiation.

In our validation study snow depth data were simulated for $\varepsilon_S = 0.99$, which is too large (compared with the real snow emissivity estimated for Wasserkuppe; see below) and therefore the albedo was overestimated. Testing a more realistic value of $\varepsilon_S = 0.90$ for simulations, the bias of the estimated albedo (jointly estimated with ε_S) was clearly reduced (cf. asterisk in Fig. 2). This finding suggests that for subalpine regions the default $\varepsilon_S = 0.99$ in ESCIMO might have to be replaced by a more adequate value. Later on we will recommend values for ε_S on the basis of a joint estimation of albedo and snow emissivity from observational data (see below).

Another clear and general result was that the error range of the albedo estimate decreased with increasing albedo. Estimations become more precise with the availability of more data that means for long spells of snow, which can be generated by repeated snow fall. In this way, long spells represent the large albedo of fresh snow ($\alpha \approx 0.8 - 0.9$ (Kraus, 2008)). Conversely, short spells of snow-cover can represent aged snow ($\alpha \approx 0.45 - 0.90$ (Kraus, 2008)).

Comparing different stations it turned out that albedo estimates

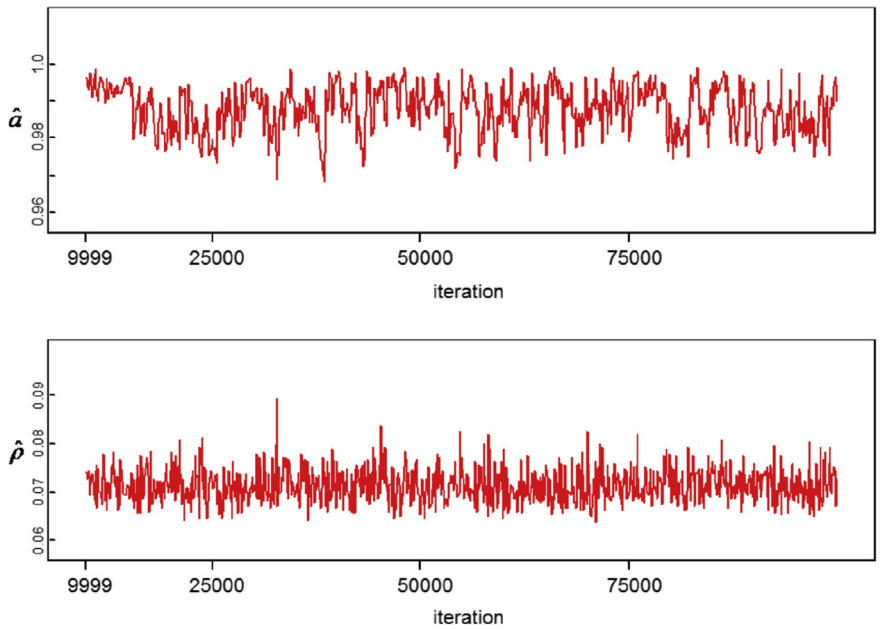

Fig. 1. Convergence of MCMC iterations for an estimation of albedo and snow density with OpenBUGS using data at Erfurt-Weimar (results were similar for the other stations; the selection of the start values did not affect the solutions).

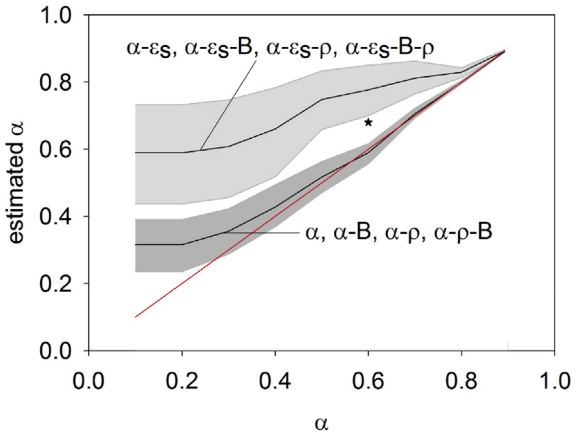

Fig. 2. Estimated albedo at Wasserkuppe (for $\varepsilon_s = 0.99,\ B = 2.0\ W/m^2,\ \rho = 0.18 g/cm^3$) depending on the albedo used for snow depth simulation and on the combination of parameter estimates. Dark lines represent the median; grey areas range from 25th to 75th percentile; red line indicates exact correspondence. All estimates cluster in two distinct groups of error ranges; the group involving snow emissivity is strongly biased to larger albedo estimates. The asterisk represents the median albedo estimated for a simulation using $\varepsilon_s = 0.9,\ \alpha = 0.6$. (For interpretation of the references to colour in this figure legend, the reader is referred to the Web version of this article.)

equal the theoretical albedo only for values larger than approximately 0.5. For $\alpha < 0.5$ the error increases and for very small albedo values the estimate was nearly independent on the albedo used for simulations (Fig. 2); this is similar in the plots for Erfurt-Weimar and Artern (not shown here). This can be understood as a consequence of the differences in the number of days without snow that was 92%, 89%, 75% in the considered time period for Artern, Erfurt-Weimar, and Wasserkuppe, respectively. For large albedo values ($\alpha \geq 0.90$) the bias vanished for all stations, even for the albedo estimated jointly with snow emissivity, and the error range diminishes to about 1%. For small albedo values ($\alpha < 0.50$) the estimation is strongly biased and therefore useless.

Though the estimates of snow density (ρ) tended to be slightly biased by a joint estimation with snow emissivity (Fig. 3), this bias was not significant because the error range included the exact agreement between theoretical and estimated values. There was a general (but also not significant) tendency to overestimate the snow density. As Wasserkuppe had more days with snow cover, the precision of the estimated snow density was higher, compared with the other stations.

The estimation of snow emissivity (ε_s) had very diverse results (Fig. 4). For Wasserkuppe all estimates cluster in three distinct groups (Fig. 4a). A joint estimation of ε_s with albedo generates an overestimation and an estimation together with snow density (but not with albedo!) generates an underestimation of the snow emissivity in the range $0.95 < \varepsilon_s < 0.96$. For Erfurt-Weimar just those estimations involving the albedo were biased towards larger snow emissivity and all others were unbiased (Fig. 4b). For the station Artern all estimations of snow emissivity were nearly not biased (Fig. 4c).

For values $\varepsilon_s > 0.92$ the estimation of snow emissivity was only slightly biased. Our simulations confirm the above observation that estimates of albedo and snow emissivity interact. Therefore the accuracy of snow emissivity estimations might be improved for other values of the albedo.

An aim of the present study was to demonstrate the usefulness of Bayesian inference for snow depth modelling. To illustrate the advantage of the Bayesian approach over the maximum likelihood method the latter was used as an alternative to estimate the parameter snow emissivity (ε_s) for the station Wasserkuppe. For the estimation of this parameter and the situation of snow cover ($SD > 0$) without any snow or rain ($S = R = 0$) equations (1–12) can be reformulated to a generalized regression model. This regression with offset involves an exponential distribution of the snow depth $SD_t \sim \exp(\lambda_t)$. Given $\rho = 0.1\ g/cm^3$ and the daily values of $SD_t,\ \vartheta_t,\ relHum_t,\ u_t$, an estimate of the snow emissivity can be calculated (e.g. in R using glm with Gamma distribution as generalization of the exponential and with inverse link function) and results in $\widehat{\varepsilon}_s = 1.11 \pm 0.14 \in [0.97, 1.25]$. Maximum likelihood estimators approximately follow a normal distribution. This interval estimate does not comply with the restriction $0 \leq \varepsilon_s \leq 1$, however.

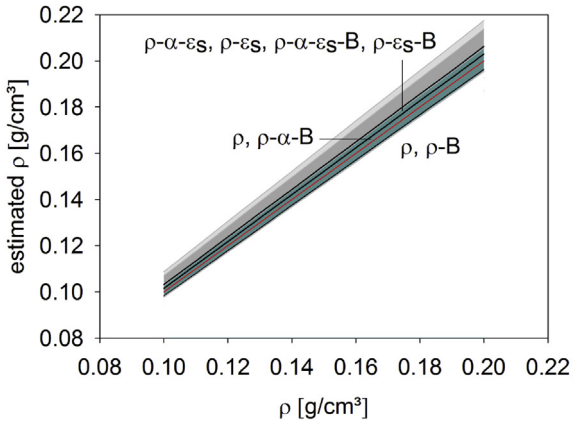

Fig. 3. Estimated snow density at Wasserkuppe (for $\alpha = 0.90$, $\varepsilon_s = 0.99$, $B = 2.0\ W/m^2$) depending on the snow density used for snow depth simulation and on the combination of parameter estimates. Dark lines represent the median; grey areas range from 25th to 75th percentile; red line represents exact correspondence. (For interpretation of the references to colour in this figure legend, the reader is referred to the Web version of this article.)

In contrast, the Bayesian estimate $\widehat{\varepsilon}_s = 0.99 \pm 0.01$ clearly corresponds to the value $\varepsilon_s = 0.99$ that was used to simulate the snow depths and remains in the interval $[0, 1]$ (Fig. 4a).

The estimation of the soil heat flux (B) was rather poor (Fig. 5) for all stations. There was not only bias but also a very large error range. Considering the magnitude of the energy terms in the balance equation (5), it turns out that B is smaller than all other terms by a factor of 1/10 … 1/100. Therefore minor inaccuracies of the other energy terms will have an immense impact on the estimation of the soil heat flux. Another reason for the large estimation error of B is that the soil temperature that is relevant for the soil heat flux can be different. ESCIMO assumes a soil temperature equal to the snow temperature (of 273.15 K), and this is just an approximate parameterization of the model. Further, the bias of the soil heat flux estimate towards lower values might be caused by the fact that the ESCIMO equations were used for daily time steps. Originally it was designed for hourly time steps and was able to account for reduced soil heat fluxes during the night. This makes the daily average soil heat flux smaller than the flux during daytime.

Summarizing our validation study of all the four considered parameters, we conclude that snow density was estimated most accurately and this is in agreement with the stable solution of the MCMC simulation (Fig. 1). In contrast, the estimation of soil heat flux was very poor. Albedo and snow emissivity estimates interact and this suggests making a joint estimation in order to have reasonable values for both.

4.2. Parameter estimation from observational data

In an application of the suggested inverse modelling procedure the four parameters (α, ρ, ε_s, B) were estimated from real snow depth data recorded at three stations during 2.5 years (August 2010–December 2012). For each station all parameters have been estimated in different combinations. At the beginning, each parameter was estimated alone and the other parameters were set to fixed values. This was completed by pairs and triples of parameter estimates; finally all four parameters were estimated jointly and this procedure resulted in consistent estimates.

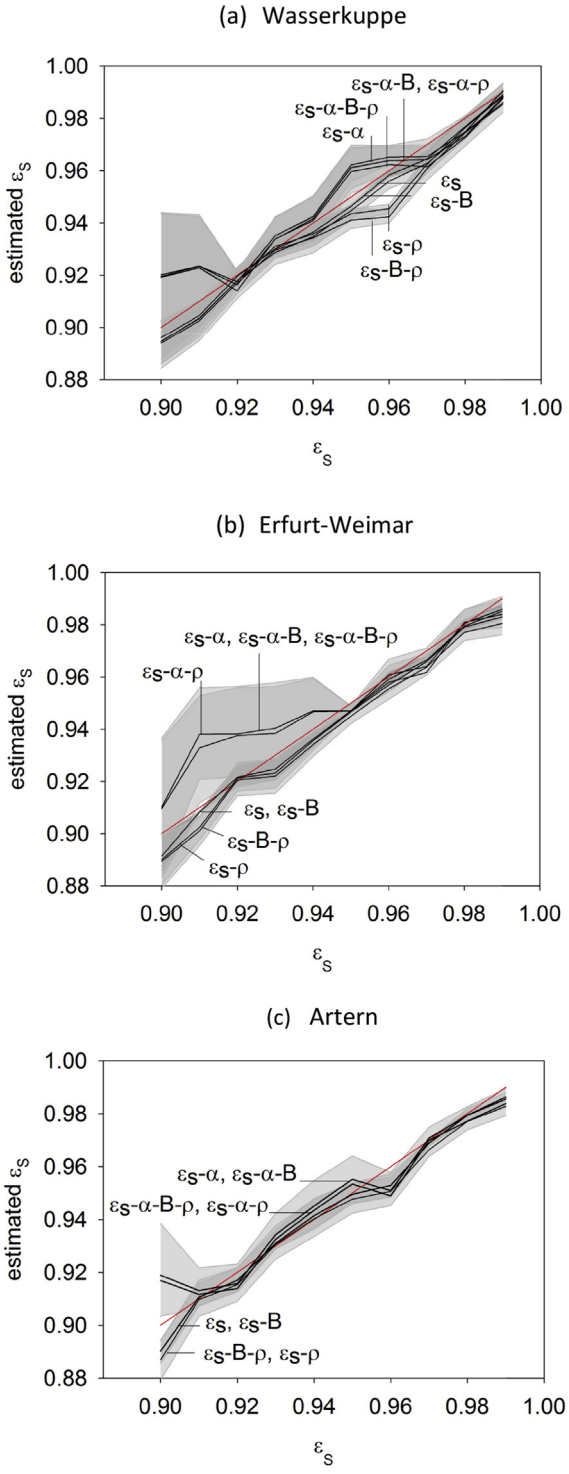

Fig. 4. Estimated snow emissivity at Wasserkuppe (a, for $\rho = 0.18 g/cm^3$), Erfurt-Weimar (b, for $\rho = 0.13 g/cm^3$), and Artern (c, for $\rho = 0.10 g/cm^3$) (all with $\alpha = 0.90$, $B = 2.0\ W/m^2$) depending on the snow emissivity used for snow depth simulation and on the combination of parameter estimates. Dark lines represent the median; grey areas range from 25th to 75th percentile; red line represents exact correspondence. (For interpretation of the references to colour in this figure legend, the reader is referred to the Web version of this article.)

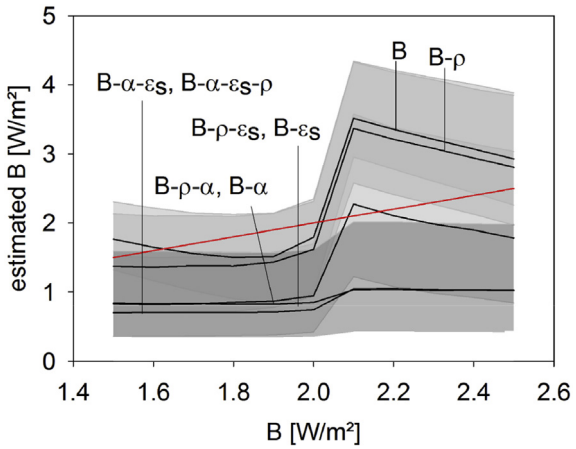

Fig. 5. Estimated soil heat flux at station Wasserkuppe (for $\alpha = 0.90$, $\rho = 0.18 g/cm^3$, $\varepsilon_s = 0.99$) depending on the soil heat flux used for snow depth simulation and on the combination of parameter estimates. Dark lines represent the median; grey areas range from 25th to 75th percentile; red line represents exact correspondence. (For interpretation of the references to colour in this figure legend, the reader is referred to the Web version of this article.)

Extending the original ESCIMO model that calculates the snow water equivalent (*SWE*), here the snow depth (*SD*) was modelled directly. The application study demonstrated that the ratio *SWE*/*SD* significantly depends on the state of the snow cover and, therefore, different snow densities were included for new snow (ρ_o), for melting snow (ρ_M), for sublimated snow (ρ_s), and for frozen rain on snow cover (ρ_r) into the mass balance (eq. (2)). All snow densities are limited in their value by the density of ice that is $\rho_{ice} = 0.918\, g/cm^3$ and this was taken into account in the inverse modelling approach. Joint estimations of the four densities always resulted in $\widehat{\rho}_s = \widehat{\rho}_r = \widehat{\rho}_M = \rho_{ice}$. Generally the estimated density of new snow was lower than for ice ($\widehat{\rho}_o < \rho_{ice}$); even for aged snow covered by firn or ice the density was below $0.6\, g/cm^3$.

An estimation of the snow density from observational data (Table 2) resulted in station-specific values of $\widehat{\rho}_o \approx 0.14\, g/cm^3$ and $\widehat{\rho}_o \approx 0.05\, g/cm^3$ for Wasserkuppe and Erfurt-Weimar, respectively. For Artern the snow density was consistently estimated as $\widehat{\rho}_o \approx 0.11\, g/cm^3$. Obviously, the snow density increases with the accumulation and ageing of snow and this occurs more likely at a mountain station (Wasserkuppe) as opposed to an urban lowland station (Erfurt-Weimar) where the time of snow cover is reduced due to urban heat island effects.

The snow emissivity $\widehat{\varepsilon}_s$ varied between stations (Table 2). The estimation of the soil heat flux $\widehat{B}$ was very uncertain as a consequence of the dominance of the other parts in the energy balance. Nevertheless, our estimations indicated that a value of $\widehat{B} \approx 1.0 W/m^2$ is reasonable for the soil heat flux in our study region; the default value in ESCIMO was 2.0 W/m^2. All achieved estimates are summarized in Table 2 as a recommendation for the application in ESCIMO with data relevant for sub-alpine regions.

The estimated albedo was site specific and decreased from Wasserkuppe ($\widehat{\alpha} \approx 0.94$) to Erfurt-Weimar ($\widehat{\alpha} \approx 0.89$) to Artern ($\widehat{\alpha} \approx 0.56$). These changes in the albedo correspond to the changes in the altitude of these stations (921 *m*, 316 *m*, 164 *m*) a.s.l. Stations at higher altitudes experience new snowfall more often and this is associated with a larger albedo. Strasser and Marke (2010) used albedo values between 0.45 and 0.90. Combining albedometer measurements with Landsat TM images for an alpine glacier, Strasser et al. (2004) developed an exponential decay parameterization of the albedo $\alpha = \alpha_{\min} + \alpha_{add} \cdot e^{-kn}$ with n representing the number of days since the last considerable snowfall (i.e. at least $SWE = 0.5\ mm/h$) which caused an increase of the snow albedo to its maximum value $\alpha_{\min} + \alpha_{add}$ ($\alpha_{\min}$ is the minimum albedo of (old) snow, α_{add} is an additive albedo and k is a recession factor that is defined as −0.12 for positive temperatures and −0.05 for negative temperatures (Strasser and Marke, 2010),).

This parameterization was also used in ESCIMO and specifies the maximum albedo to 0.95, but this level can be clearly exceeded by fresh snow in alpine regions (Fig. 17 in Strasser et al. (2004)). Our results for sub-alpine stations suggested that the albedo was often below this level. Further, for our stations the additive albedo changes were not significant (Table 2).

An important observation is that the albedo estimation is based on the energy balance (eq. (5)) of the ESCIMO model and this energy balance is involved merely in the amount of melting snow (eq. (4)). That means albedo estimates are(calculated only from observational data that refer to melting and, therefore, $\widehat{\alpha}$ is the albedo of melting snow. For new snow an estimation of α is not possible using the ESCIMO approach (1-12). This fact explains the unexpected small values of $\widehat{\alpha}$ and the insignificance of the snow ageing obtained from our observational data.

4.3. Assessment of forecasting performance

Assessing the quality of the parameters estimated by an inverse modelling of the 2.5 years observational data ($SD^{(o)}$), predictions ($SD^{(p)}$) were calculated for 2.5-years and 51-years periods. While the former demonstrates the precision of model fit, the latter represents the model's ability for generalization. Following performance measures were applied:

coefficient of determination

$$R^2 = \left(\frac{\sum_{t=1}^{n} \left(SD_t^{(o)} - \overline{SD^{(o)}} \right) \cdot \left(SD_t^{(p)} - \overline{SD^{(p)}} \right)}{\sqrt{\sum_{i=1}^{n} \left(SD_i^{(o)} - \overline{SD^{(o)}} \right)^2} \cdot \sqrt{\sum_{k=1}^{n} \left(SD_k^{(p)} - \overline{SD^{(p)}} \right)^2}} \right)^2, \quad (16)$$

Table 2
Parameter values jointly estimated from measured snow depth data (generally $B = 1\ W/m^2$, and $\rho_s = \rho_r = \rho_M = 0.918\ g/cm^3$,).

Parameter estimated	Wasserkuppe (921 m a.s.l.)	Erfurt-Weimar (316 m a.s.l.)	Artern (164 m a.s.l.)
$\widehat{\alpha}$	0.94 ± 0.04	0.89 ± 0.05	0.56 ± 0.04
$\widehat{\alpha}_{\min}$;	0.93 ± 0.05;	0.89 ± 0.08;	0.52 ± 0.06;
$\widehat{\alpha}_{add}$	0.03 ± 0.03	0.04 ± 0.06	0.05 ± 0.05
$\widehat{\rho}_o$ [g/cm^3]	0.14 ± 0.02	0.05 ± 0.01	0.11 ± 0.02
$\widehat{\varepsilon}_s$	0.88 ± 0.01	0.92 ± 0.03	0.99 ± 0.01

index of agreement

$$IA = 1 - \frac{\sum_{t=1}^{n}(SD_t^{(o)} - SD_t^{(p)})^2}{\sum_{i=1}^{n}\left(\left|SD_i^{(p)} - \overline{SD^{(o)}}\right| + \left|SD_i^{(o)} - \overline{SD^{(o)}}\right|\right)^2}, \quad (17)$$

and root means square error

$$RMSE = \sqrt{(1/n)\sum_{t=1}^{n}(SD_t^{(o)} - SD_t^{(p)})^2}\ , \quad (18)$$

mean absolute error

$$MAE = (1/n)\sum_{t=1}^{n}|SD_t^{(o)} - SD_t^{(p)}|\ , \quad (19)$$

mean bias error

$$MBE = (1/n)\sum_{t=1}^{n}(SD_t^{(o)} - SD_t^{(p)})\ , \quad (20)$$

and fractional bias error

$$FBE = \frac{\sum_{t=1}^{n}(SD_t^{(o)} - SD_t^{(p)})}{0.5\cdot\sum_{i=1}^{n}(SD_i^{(o)} + SD_t^{(p)})}. \quad (21)$$

R^2 measures the percentage of variance in observed snow depths explained by the statistical model, but R^2 is not able to assess a bias between observed and predicted data (Willmott, 1982; Willmott et al., 1985). For a more comprehensive evaluation the index of agreement ($IA \in (0,1)$) was included that indicates a perfect prediction for $IA = 1$. *MAE*, *MBE*, and *FBE* indicate systematic errors. The parameter values achieved from the Bayesian estimation procedure (summarized in Table 2) were used for snow depth predictions and an assessment of their quality (Table 3).

Results suggest that the performance was clearly improved for the parameter values estimated by the suggested Bayesian procedure, referring to the 2.5-years period. Predictions for the 51-years period were slightly less precise. A conclusion is that the parameter estimation can be recommended for each specific site before ESCIMO is used to forecast the snow depth at this site. The sensitivity of forecasting performance on the soil heat flux was very low.

5. Conclusions and limitations

The ESCIMO model was utilized for an inverse approach estimating the model parameters from meteorological data gathered at three stations situated in the Central German Uplands. Responding to our research hypotheses, we conclude that inverse modelling is suitable to estimate model parameters and to calculate predictions for snow depths at sub-alpine sites with urban influences which are so far underrepresented in the scientific literature. To compare and generalize the results, parameter estimation is desirable for other sub-alpine regions. While the German Weather Service (DWD) runs 52 climate stations in Thuringia (including Wasserkuppe that is located near the border), only 5 stations have complete datasets and only 3 (that represent different elevation zones) were selected for the present study. ESCIMO needs daily values for air temperature and humidity, air pressure, precipitation, wind speed, global radiation, and snow depth. Bayesian inference can handle gaps of missing data, but this will drastically increase the computing time and decrease the performance. For that reason the suggested procedure might be not feasible at many sub-alpine stations.

Extending the ESCIMO code from the snow water equivalent to the snow depth, we introduced snow densities for new snow, melting snow, sublimated snow, and frozen rain on snow cover as new parameters that need to be estimated. These additional parameter estimations are required because routine measurements provide just snow depths and the snow density can vary in time and space. Observational data of snow density are rare (recently Pohl et al. (2014) applied a sensor network for snow density measurements) and therefore an advantage of the Bayesian approach is the possibility to assess this parameter specifically for each station. This estimate provides valuable information about site-specific conditions.

The validation study (section 4.1) clearly demonstrated how the parameter estimates are mutually correlated and, therefore, a joint estimation of all parameters is recommended. This procedure guarantees that all parameter values are adequate to the prevailing state of the snow cover. The estimated site-specific parameters improve the predictions of ESCIMO compared to the use of default parameter values suggested with ESCIMO.spread (see Table 3). The occurrence of site-specific values for the parameters confirmed that the accumulation of snow depends on the altitude and the urban or mountain characteristic of a station.

In hydrological applications of snow models (such as the U.S. National Weather Service's model SNOW-17 (Anderson, 2006)), Bayesian techniques are often utilized to predict the snow water equivalent (SWE) together with the extent of the snow covered area (SCA). For that purpose data assimilation techniques (such as ensemble Kalman filter, ensemble square root filter, or particle filter) have been developed that utilize in situ (e.g., snow pillows) and remotely sensed (e.g., the Normalized Snow Density Index calculated from satellite images) measurements to improve model predictions (Leisenring and Moradkhani, 2011). As all these measurements are subject to uncertainties, sequential Bayesian updating can stochastically combine measurements with model simulations and, in this way, estimate the probability distributions of the filters' state variables. Leisenring and Moradkhani (2011) found a data assimilation performance of $RMSE = 29 - 51mm$ for their modelled *SWE* (in mm).

Assimilating Landsat 8 data with the output of the seNorge snow model (Saloranta, 2016), Stigter et al. (2017) calculated spatiotemporal predictions of SWE with a resolution of 100 m and a daily time step for their alpine study area in the central Himalayas. They used snow albedo values of 0.713 (Brock et al., 2000) and applied two different albedo decay models (logarithmic decay for deep snow $SWE \geq 5mm$; exponential decay for shallow snow $SWE < 5mm$). The present study demonstrates the very different situation under sub-alpine conditions where the estimated albedo varied between 0.56 and 0.94, and the decay was statistically not significant. While Saloranta (2014) specified the minimum snow density to 0.05 g/cm^3 for seNorge predictions of SWE and Hopfinger (1983) the density of avalanching snow to 0.2 g/cm^3, for the sub-alpine stations with urban impact we find snow densities of 0.05–0.14 g/cm^3.

Stigter et al. (2017) used the optimized seNorge model to calculate *ex post* predictions of snow depth and compare them with past observations for their Himalaya study region. The forecasting accuracy varied between $RMSE = 49mm$ for a region where snow depths are up to $400mm$ and $RMSE = 314mm$ for a region where snow depths can reach $2000mm$. The present study resulted in a forecasting accuracy between $RMSE = 308mm$ for Wasserkuppe (snow depths up to $2500mm$) and $RMSE = 43.4mm$ for Arten (snow depths lower than $400mm$).

The performance measures (Table 3) indicate that the generalization of the model is reasonable: the precision measured by R^2, *IA*, and *RMSE* is not reduced when the parameters estimated from 2.5 years of observational data are used to predict the snow depths during 51 years. In contrast, the accuracy of the forecasts is reduced when the default parameter values (derived in alpine snow studies)

Table 3
Performance measures of forecasts based on different sets of parameters (default values are used to forecast the 2.5-years period in the first three lines; Bayesian estimates are used in light grey lines to predict the 2.5-years period and in dark grey lines for the 51-years period).

	R^2	*IA*	*RMSE* cm	*MAE* cm	*MBE* cm	*FBE*
Wasserkuppe; default parameters; 2.5 years $\alpha=0.90,\ \rho_M=\rho_r=\rho_s=0.918\mathrm{g/cm^3},\ \rho_o=0.05\mathrm{g/cm^3},\varepsilon_s=0.99,\ B=2.0\,W/m^2$	0.324	0.0896	259	159	-159	-1.85
Erfurt-Weimar; default parameters; 2.5 years $\alpha=0.90,\ \rho_M=\rho_r=\rho_s=0.918\mathrm{g/cm^3},\ \rho_o=0.05\mathrm{g/cm^3},\varepsilon_s=0.99,\ B=2.0\,W/m^2$	0.634	0.303	41.7	16.1	-16.1	-1.68
Artern; default parameters; 2.5 years $\alpha=0.90,\ \rho_M=\rho_r=\rho_s=0.918\mathrm{g/cm^3},\ \rho_o=0.05\mathrm{g/cm^3},\varepsilon_s=0.99,\ B=2.0\,W/m^2$	0.64	0.312	20.6	6.98	-6.98	-1.63
Wasserkuppe; Table 2; 2.5 years $\alpha=0.94,\ \rho_M=\rho_r=\rho_s=0.918\mathrm{g/cm^3},\ \rho_o=0.14\,\mathrm{g/cm^3},\varepsilon_s=0.88,\ B=1.0\,W/m^2$	0.631	0.608	30.8	13.9	-12.8	-0.989
Erfurt-Weimar; Table 2; 2.5 years $\alpha=0.89,\ \rho_M=\rho_r=\rho_s=0.918\mathrm{g/cm^3},\ \rho_o=0.05\,\mathrm{g/cm^3},\varepsilon_s=0.92,\ B=1.0\,W/m^2$	0.73	0.404	31.7	11.3	-11.2	-1.57
Artern; Table 2; 2.5 years $\alpha=0.56,\ \rho_M=\rho_r=\rho_s=0.918\mathrm{g/cm^3},\ \rho_o=0.11\,\mathrm{g/cm^3},\varepsilon_s=0.99,\ B=1.0\,W/m^2$	0.845	0.801	4.34	1.02	-0.804	-0.678
Wasserkuppe; Table 2; 51 years $\alpha=0.94,\ \rho_M=\rho_r=\rho_s=0.918\mathrm{g/cm^3},\ \rho_o=0.14\,\mathrm{g/cm^3},\varepsilon_s=0.88,\ B=1.0\,W/m^2$	0.578	0.591	32.4	13.4	-12.1	-0.917
Erfurt-Weimar; Table 2; 51 years $\alpha=0.89,\ \rho_M=\rho_r=\rho_s=0.918\mathrm{g/cm^3},\ \rho_o=0.05\,\mathrm{g/cm^3},\varepsilon_s=0.92,\ B=1.0\,W/m^2$	0.56	0.33	17.3	5.41	-5.34	-1.51
Artern; Table 2; 51 years $\alpha=0.56,\ \rho_M=\rho_r=\rho_s=0.918\mathrm{g/cm^3},\ \rho_o=0.11\,\mathrm{g/cm^3},\varepsilon_s=0.99,\ B=1.0\,W/m^2$	0.709	0.782	2.91	0.709	-0.46	-0.557

are used (cf. the extremely large *RMSE* for Wasserkuppe). The always negative values for *MBE* and *FBE* indicate that the model predictions are biased to lower snow depths.

Improvements are needed for the estimation of the soil heat flux. The parameterization applied in ESCIMO is rather simple and an involvement of the soil temperature profile might be beneficial. Possibly, the chosen exponential prior is not optimal and might be improved. A third problem to be solved with the estimation of B arises from its small value compared to the other terms in the energy balance.

Originally, ESCIMO was developed for hourly time steps (Strasser and Marke, 2010). For compatibility with observed meteorological data, for which only daily data were available, we modified the time-base of ESCIMO from hourly to daily time steps and this might have an impact on the interpretation of the parameter values. Especially the parameters α, ρ_o, ε_s, B studied here represent daily values, while, in the original ESCIMO code, they can vary during the day. This means, the parameters on a daily basis are certain averages of these hourly data and are attenuated in their extremes. For example, the ageing of snow appears smoothed in the daily parameters. Nevertheless, ESCIMO proved to be applicable to both hourly and daily data. As ESCIMO is a physically based point snow surface model, all estimated parameters refer to the location where the data have been gathered. Our approach provides point values of snow density, albedo, snow emissivity, and soil heat flux. The model does not give any information about the changes of these parameters along the snow surface and with increasing distance to the observation site.

The extension of the original ESCIMO model by a parameterization of the long-wave radiation (eq. (11 + 12)) proved to be beneficial, as this made the presented inverse model applicable with routine monitoring data from which long-wave radiation is often not available. Including parameters for snow densities into the original ESCIMO model considerably improved the performance of the model because these parameters are mostly not available at the monitoring sites. Even the snow prediction for new datasets takes advantage of the parameters estimated by the inverse model. Another extension of ESCIMO was recently suggested by (Marke et al., 2016), who advance the model to inside-canopy conditions.

6. Software and data availability

The study is based on data gathered in the frame of the regional climate information system ReKIS. They were freely downloaded as text files from www.rekis.org for the stations Wasserkuppe, Erfurt-Weimar, and Artern as daily values for a period of 51 years (January 1st, 1961 until December 31st, 2012). For all calculations the free language R for statistical computing (www.r-project.org) was used. For Bayesian inference the software OpenBUGS (BUGS = Bayesian

inference using Gibbs Sampling (Ntzoufras, 2011)) is based on the Markov Chain Monte Carlo (MCMC) method (Gelfand and Smith, 1990) and is freely available at www.openbugs.net where all further information is provided. The code for the inverse model developed by the authors is provided in the supporting material.

Acknowledgements:

The authors are grateful to Frank Heyner (Klimaagentur Thüringen, Thüringer Landesanstalt für Umwelt und Geologie – TLUG) for inspiring discussions and help with the data needed for the performance assessment. D. H. was financially supported by the Deutsche Bundesstiftung Umwelt (DBU), Osnabrück (AZ: 20015/373).

Appendix A. Supplementary data

Supplementary data related to this article can be found at https://doi.org/10.1016/j.envsoft.2018.01.010.

References

Anderson, E.A., 2006. Snow accumulation and ablation model. NWSRFS (National weather Service river forecast system). Snow17 2005. II.2-SNOW-17: HYDRO-17 Snow Model, User Manual for Release 81. http://www.weather.gov/oh/hrl//nwsrfs/users_manual/part2/_pdf/22snow17.pdf.

Aster, R.C., Borchers, B., Thurber, C.H., 2013. Parameter Estimation and Inverse Problems, second ed. Elsevier AP, Amsterdam ; Heidelberg [u.a.]. ed.

Atwater, M.A., Brown, P.S., 1974. Numerical computations of latitudinal variation of solar-radiation for an atmosphere of varying opacity. J. Appl. Meteorol. 13 (2), 289–297.

Bartelt, P., Lehning, M., 2002. A physical SNOWPACK model for the Swiss avalanche warning Part I: numerical model. Cold Reg. Sci. Technol. 35 (3), 123–145.

Brock, B.W., Willis, I.C., Sharp, M.J., 2000. Measurement and parameterization of albedo variations at Haut Glacier d'Arolla, Switzerland. J. Glaciol. 46 (155), 675–688.

Crawford, T.M., Duchon, C.E., 1999. An improved parameterization for estimating effective atmospheric emissivity for use in calculating daytime down welling longwave radiation. J. Appl. Meteorol. 38 (4), 474–480.

Etchevers, P., Martin, E., Brown, R., Fierz, C., Lejeune, Y., Bazile, E., Boone, A., Dai, Y., Essery, R., Fernandez, A., Gusev, Y., Jordan, R., Koren, V., Kowalcyzk, E., Nasonova, N.O., Pyles, R.D., Schlosser, A., Shmakin, A.B., Smirnova, T.G., Strasser, U., Verseghy, D., Yamazaki, T., Yang, Z.L., 2004. Validation of the energy budget of an alpine snowpack simulated by several snow models (SnowMIP project). In: Fohn, P.M.B. (Ed.), Annals of Glaciology, vol. 38, pp. 150–158, 2004.

Gelfand, A.E., Smith, A.F.M., 1990. Sampling-based approaches to calculating marginal densities. J. Am. Stat. Assoc. 85 (410), 398–409.

Hess, P., Brezowsky, H., 1969. Katalog der Grosswetterlagen Europas, 2. neubearbeitete und ergänzte Aufl. Berichte des Deutschen Wetterdienstes 113. Bd. 15. Deutscher Wetterdienst, Offenbach am Main.

Hopfinger, E.J., 1983. Snow avalanche motion and related phenomena. Annu. Rev. Fluid Mech. 15, 47–76.

Kraus, H., 2008. Grundlagen der Grenzschicht-Meteorologie: Einführung in die Physik der Atmosphärischen Grenzschicht und in die Mikrometeorologie. Springer.

Kuchment, L.S., Gelfan, A.N., 1996. The determination of the snowmelt rate and the meltwater outflow from a snowpack for modelling river runoff generation. J. Hydrol. 179 (1–4), 23–36.

Lamb, H.H., 1950. Types and spells of weather around the year in the british-isles - annual trends, seasonal structure of the year, singularities. Q. J. R. Meteorol. Soc. 76 (330), 393–438.

Leisenring, M., Moradkhani, H., 2011. Snow water equivalent prediction using Bayesian data assimilation methods. Stoch. Environ. Res. Risk Assess. 25 (2), 253–270.

Lunn, D., Spiegelhalter, D., Thomas, A., Best, N., 2009. The BUGS project: evolution, critique and future directions. Stat. Med. 28 (25), 3049–3067.

Marke, T., Mair, E., Forster, K., Hanzer, F., Garvelmann, J., Pohl, S., Warscher, M., Strasser, U., 2016. ESCIMO.spread (v2): parameterization of a spreadsheet-based energy balance snow model for inside-canopy conditions. Geosci. Model Dev. (GMD) 9 (2), 633–646.

Marke, T., Strasser, U., Hanzer, F., Stotter, J., Wilcke, R.A.I., Gobiet, A., 2015. Scenarios of future snow conditions in Styria (Austrian Alps). J. Hydrometeorol. 16 (1), 261–277.

Mauser, W., Bach, H., 2009. PROMET - large scale distributed hydrological modelling to study the impact of climate change on the water flows of mountain watersheds. J. Hydrol. 376 (3–4), 362–377.

McDonald, J.E., 1960. Direct absorption of solar radiation by atmospheric water vapor. J. Meteorol. 17 (3), 319–328.

Meyers, T.P., Dale, R.F., 1983. Predicting daily insolation with hourly cloud height and coverage. J. Clim. Appl. Meteorol. 22 (4), 537–545.

Ntzoufras, I., 2011. Bayesian Modeling Using WinBUGS. John Wiley & Sons.

Pohl, S., Garvelmann, J., Wawerla, J., Weiler, M., 2014. Potential of a low-cost sensor network to understand the spatial and temporal dynamics of a mountain snow cover. Water Resour. Res. 50 (3), 2533–2550.

Prata, A.J., 1996. A new long-wave formula for estimating downward clear-sky radiation at the surface. Q. J. R. Meteorol. Soc. 122 (533), 1127–1151.

R Core Team, 2014. R: a language and environment for statistical computing. R Foundation for Statistical Computing, Vienna, Austria.

Saloranta, T.M., 2014. Simulating more accurate snow maps for Norway with MCMC parameter estimation method. Cryosphere Discuss. 2014, 1973–2003.

Saloranta, T.M., 2016. Operational snow mapping with simplified data assimilation using the seNorge snow model. J. Hydrol. 538, 314–325.

Schmidt, P., Steiger, R., Matzarakis, A., 2012. Artificial snowmaking possibilities and climate change based on regional climate modeling in the Southern Black Forest. Meteorol. Z. 21 (2), 167–172.

Spiegelhalter, D., Rice, K., 2009. Bayesian statistics. Scholarpedia 4, 5230.

Stigter, E.E., Wanders, N., Saloranta, T.M., Shea, J.M., Bierkens, M.F.P., Immerzeel, W.W., 2017. Assimilation of snow cover and snow depth into a snow model to estimate snow water equivalent and snowmelt runoff in a Himalayan catchment. Cryosphere 11 (4), 1647–1664.

Strasser, U., Corripio, J., Pellicciotti, F., Burlando, P., Brock, B., Funk, M., 2004. Spatial and temporal variability of meteorological variables at Haut Glacier d'Arolla (Switzerland) during the ablation season 2001: measurements and simulations. Journal of Geophysical Research-Atmospheres 109 (D3).

Strasser, U., Etchevers, P., Lejeune, Y., 2002. Inter-comparison of two snow models with different complexity using data from an alpine site. Nordic Hydrology 33 (1), 15–26.

Strasser, U., Marke, T., 2010. ESCIMO.spread - a spreadsheet-based point snow surface energy balance model to calculate hourly snow water equivalent and melt rates for historical and changing climate conditions. Geosci. Model Dev. (GMD) 3 (2), 643–652.

Sturm, M., Taras, B., Liston, G.E., Derksen, C., Jonas, T., Lea, J., 2010. Estimating snow water equivalent using snow depth data and climate Classes. J. Hydrometeorol. 11 (6), 1380–1394.

Vionnet, V., Brun, E., Morin, S., Boone, A., Faroux, S., Le Moigne, P., Martin, E., Willemet, J.M., 2012. The detailed snowpack scheme Crocus and its implementation in SURFEX v7.2. Geosci. Model Dev. (GMD) 5 (3), 773–791.

Willmott, C.J., 1982. Some comments on the evaluation of model performance. Bull. Am. Meteorol. Soc. 63 (11), 1309–1313.

Willmott, C.J., Ackleson, S.G., Davis, R.E., Feddema, J.J., Klink, K.M., Legates, D.R., Odonnell, J., Rowe, C.M., 1985. Statistics for the evaluation and comparison of models. Journal of Geophysical Research-Oceans 90 (NC5), 8995–9005.